Supplementary Information for

In-plane aligned doping pattern in electrospun PEI/MBene nanocomposites for high-temperature capacitive energy storage

Sidi Fan,[a] Ding Ai,[b] Wenqi Zhang,[a] Rui Yang,[a] Guangyi Shen[a], Xiao Yang,[a] Yonghong Cheng,[b]* and Xiang Yu[a]*

[a]*State Key Laboratory of Alternate Electrical Power System with Renewable Energy Sources, School of Electrical and Electronic Engineering, North China Electric Power University, Beijing 102206, China*

[b]*State Key Laboratory of Electrical Insulation and Power Equipment, School of Electrical Engineering, Xi'an Jiaotong University, Xi'an 710049, China*

* Corresponding authors.

E-mail: xiangyu@ncepu.edu.cn (X.Y); cyh@xjtu.edu.cn (Y.C)

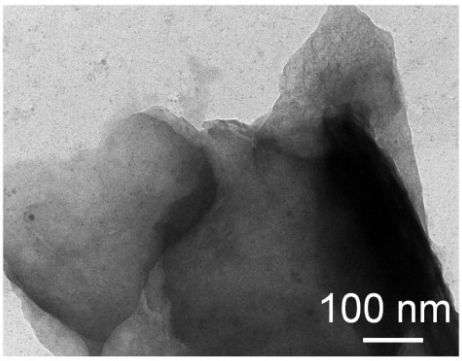

Figure S1. TEM image of MBene flakes.

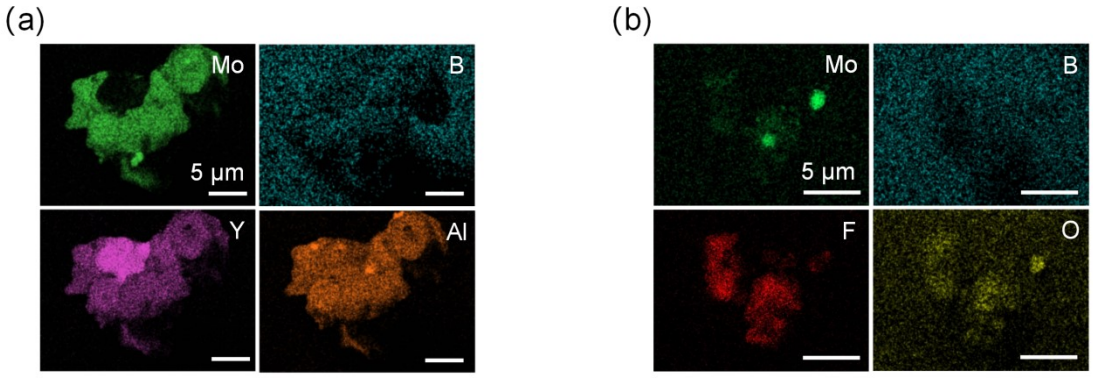

Figure S2. (a) EDS mappings of MAB phase, corresponding to flakes observed in Figure 2a; (b) EDS mappings of MBene phase, corresponding to flakes observed in Figure 2b.

Note 1. Theoretical calculations of MBene terminated with different functional groups

Density functional theory (DFT) implemented in the Vienna ab initio Simulation Package (VASP) is employed, adopting the Generalized Gradient Approximation (GGA) proposed by Perdew-Burke-Ernzerhof (PBE) for the electron exchange and correlation functional. To enhance computational accuracy, the plane-wave energy cutoff is increased to 1.3 times its original value. The standards for electronic convergence (EDIFF) is set at 0.01 meV per atom, and the atom convergence (EDIFFG) is -0.01 $eV \cdot Å^{-1}$. During structural optimization calculations, a maximum of 150 steps for electronic relaxation (NELM) and 200 steps for structural relaxation (NSW) are assigned. Once the structural optimization is finalized, a self-consistent field calculation is performed to minimize the system energy and refine the lattice structure, with NSW set to 0 to ensure that the optimization is solely applied on electrons. Highly symmetric structures are generated using vaspkit, followed by non-self-consistent calculations to analyze the density of states (DOS) and energy band structure, providing further insights into the electronic properties of MBene.

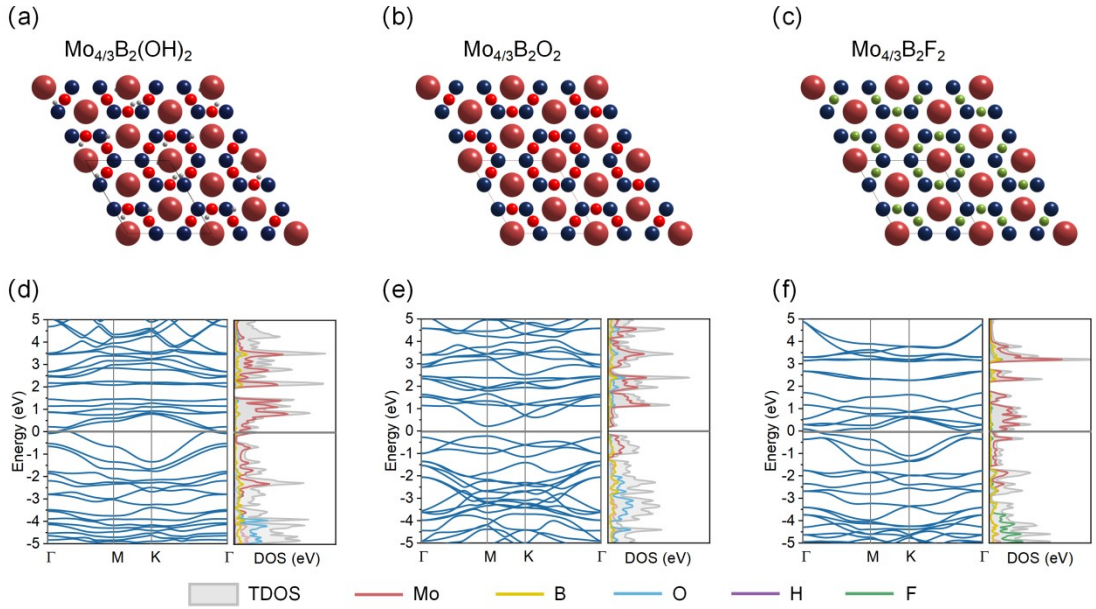

Figure S3. (a) Optimized models of MBene-OH, (b) MBene-O, and (c) MBene-F, along with their energy band structures and DOS in (e)-(f), respectively.

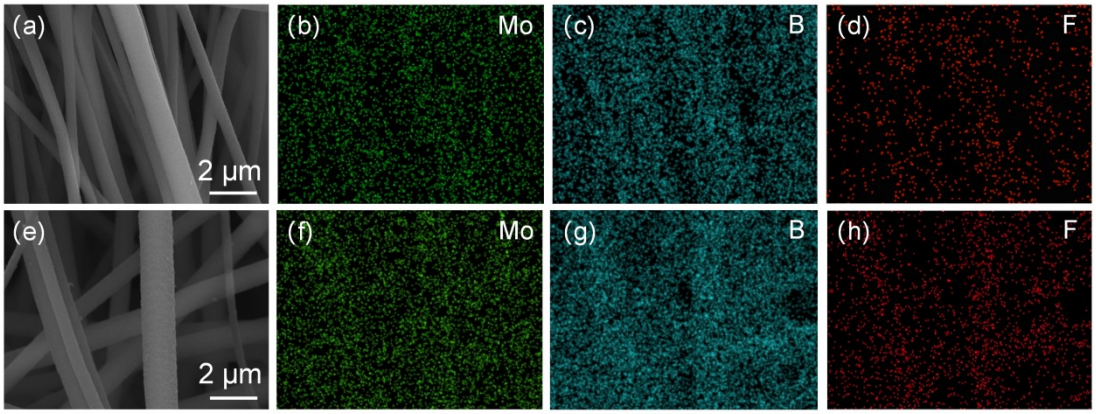

Figure S4. (a) EDS mapping of A-MBene/PEI, with individual element of (b) Mo, (c) B, and (d) F; (e) EDS mapping of R-MBene/PEI, with individual element of (f) Mo, (g) B, and (h) F.

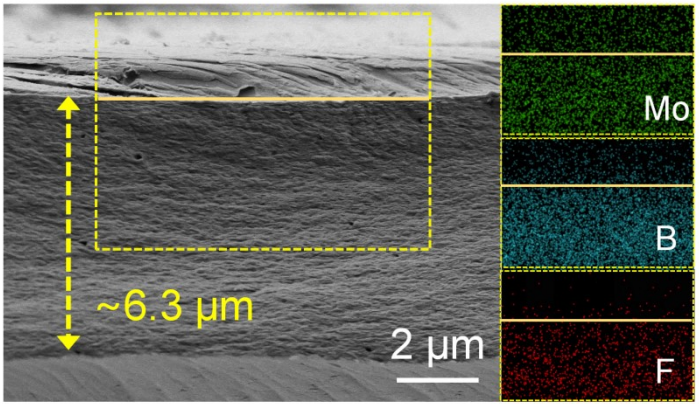

Figure S5. Cross-sectional SEM image of A-MBene/PEI (left panel), and elemental mappings of Mo, B, and F (right panel), acquired from the region marked by a yellow dashed rectangle, with a solid yellow line denoting the surface of A-MBene/PEI film.

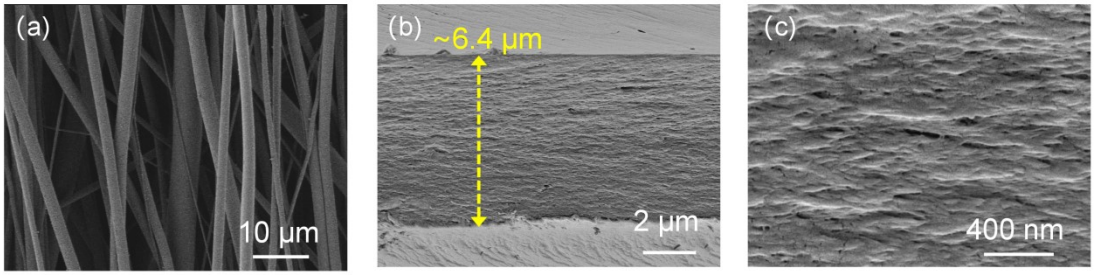

Figure S6. (a) SEM image of the electrospun PEI film before hot pressing. (b) Cross-sectional morphology of the pristine PEI film after hot pressing, with a magnified view in (c).

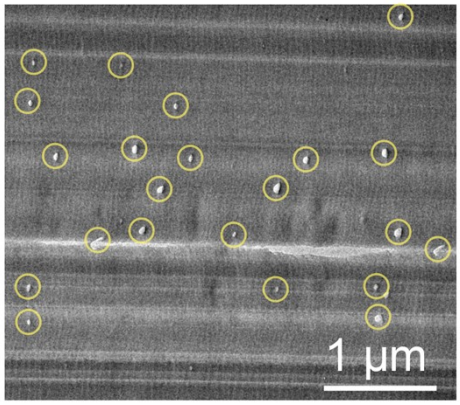

Figure S7. TEM image of A-MBene/PEI, where the MBene flakes are circled in yellow.

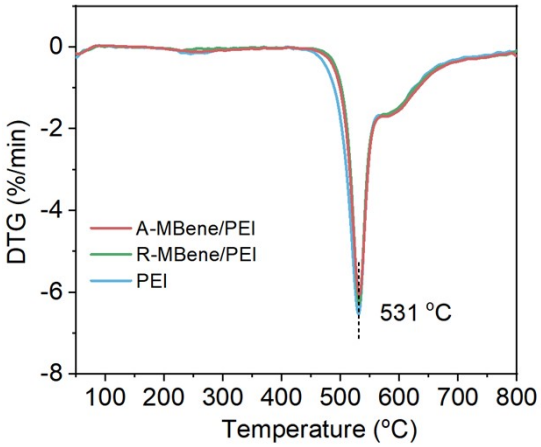

Figure S8. DTG curves of PEI, R-MBene/PEI, and A-MBene/PEI.

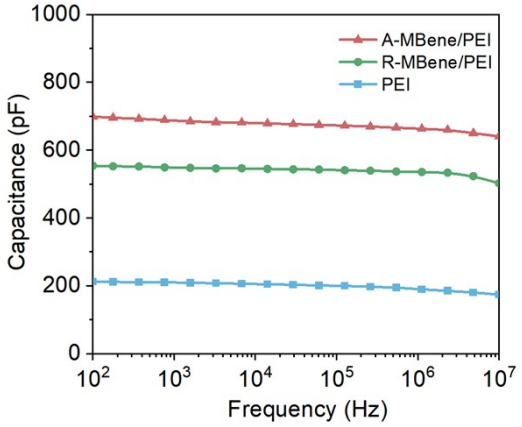

Figure S9. Frequency-dependent capacitance of various films at room temperature.

Note 2. Electric field distributions based on finite element analysis

Two models representing A-MBene/PEI and R-MBene/PEI composites are constructed using the co-simulation of COMSOL Multiphysics and MATLAB. The coding flow diagram is shown in Figure S8. As illustrated in Figure S9, a cube with a length of 2000 nm on each side is set as the PEI matrix. A specific quantity (1 wt%) of cylinders with a radius of 250 nm and a height of 50 nm is randomly dispersed in the cube, representing MBene fillers. To simulate varying degrees of filler alignments, the orientation of these fillers is adjusted. In the A-MBene/PEI model, the tilt angle between these fillers and the xy-plane is confined within 10°, while this angle is controlled to be less than 45° in the R-MBene/PEI model. Before each new filler is introduced, a traversal method is used to determine if it intersects with any of previously placed fillers. If the new filler passes this non-intersection check, it is incorporated into the packing set, and its mass is factored into the overall filler content. Once the total packing content surpasses the desired loading ratio, the final model of the composite system, with the specified filler loading, is obtained.

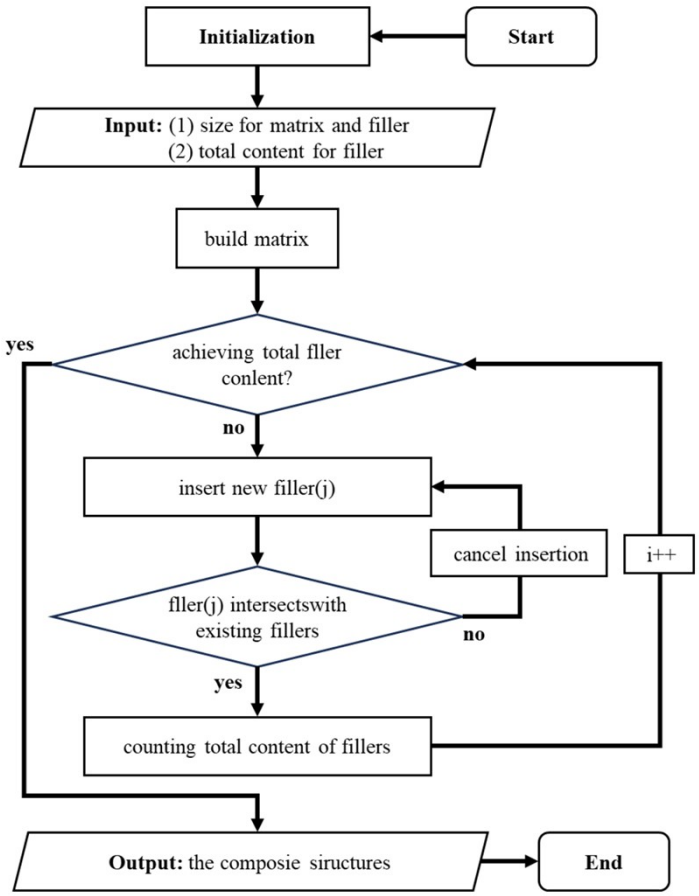

Figure S10. The code flow diagram for the model construction.

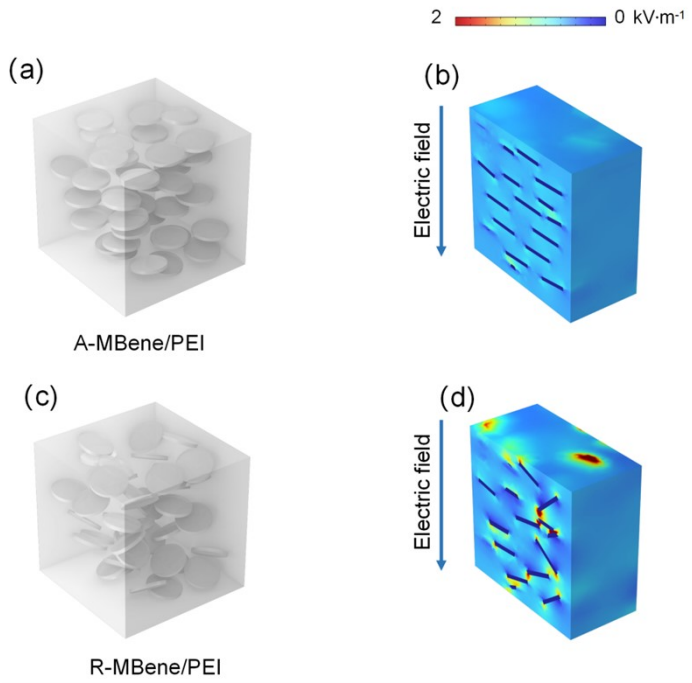

Figure S11. (a) The A-MBene/PEI composite model with its electric field distribution in (b). (c) The R-MBene/PEI composite model with its electric field distribution in (d).

The specific parameter settings are summarized in Table S1. The electrostatic model (***es***) built in COMSOL is utilized to calculate the electric field distributions. By applying a high voltage of 1 kV to the topsid of the cube, the steady-state properties of the composite system are systemically analyzed.

Table S1. The specific parameter settings for each material

Material	Density ($g \cdot cm^{-3}$)	Dielectric constant
MBene filler	6.33	3000
PEI matrix	1.27	3

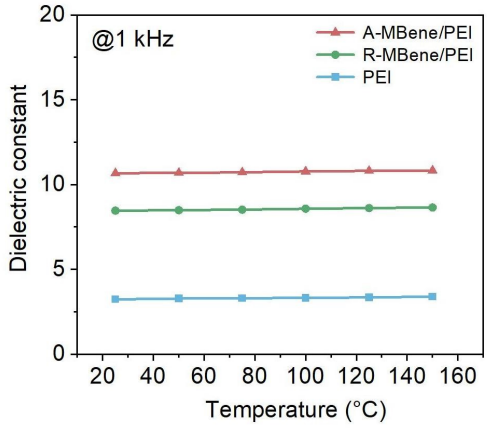

Figure S12. Temperature-dependent dielectric constant of various films at 1 kHz.

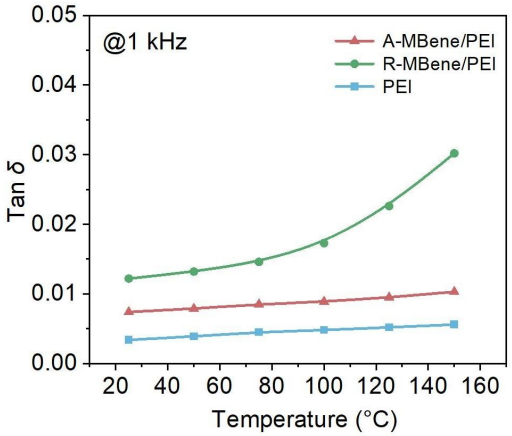

Figure S13. Temperature-dependent dielectric loss of various films at 1 kHz.

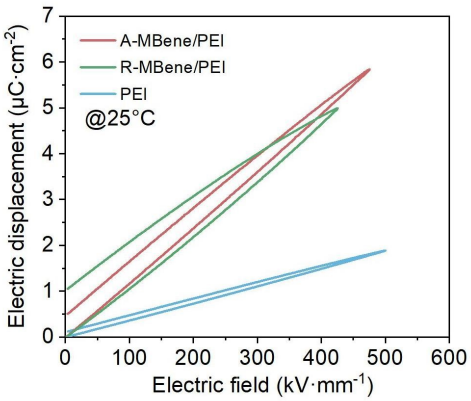

Figure S14. *D-E* loops for PEI, R-MBene/PEI, and A-MBene/PEI at room temperature.

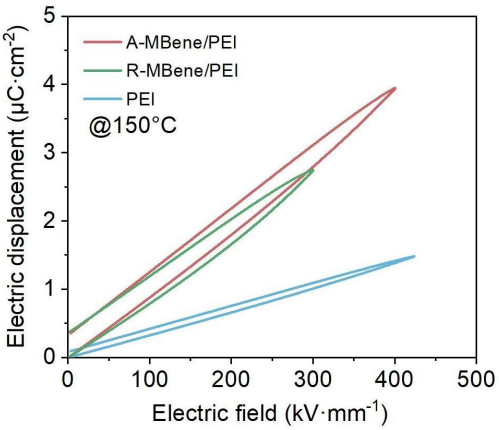

Figure S15. *D-E* loops for PEI, R-MBene/PEI, and A-MBene/PEI at 150°C.

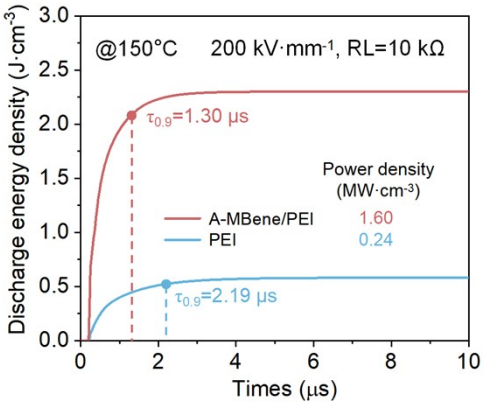

Figure S16. Discharging curves as a function of time for PEI and A-MBene/PEI

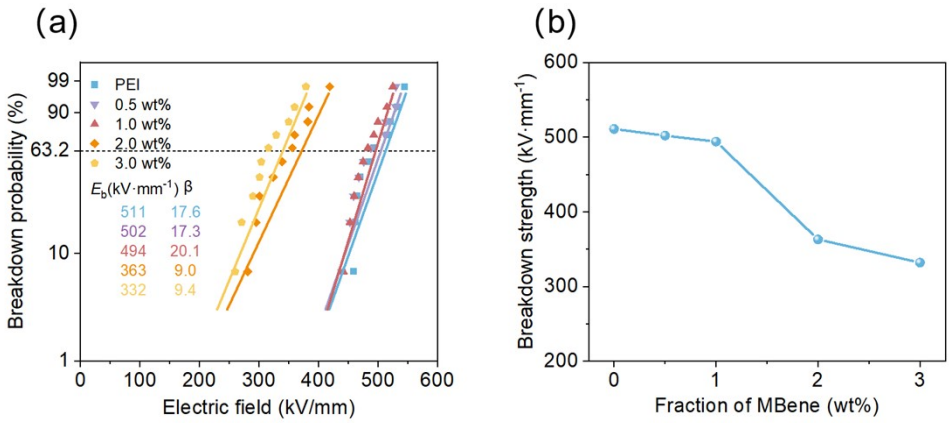

Figure S17. (a) Weibull distribution plots of A-MBene/PEI with different doping ratios. (b) E_b values of each sample.

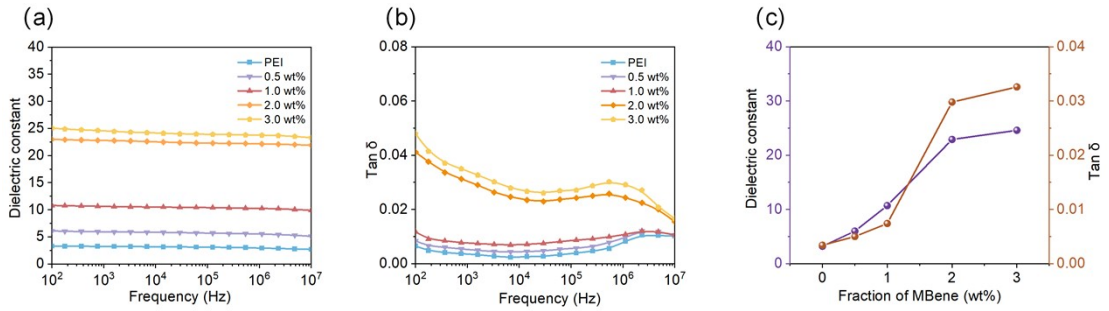

Figure S18. (a) Dielectric constant and (b) dielectric loss of A-MBene/PEI with different doping ratios. (c) A comparative analysis of dielectric parameters at 1kHz.